Research Article

Open Access Journal of Physics & Mathematics

ISSN: 3068-7527

OPENPUB GLOBAL PUBLISHERS

Received: 05-05-2025 **Accepted:** 10-05-2025 **Published:** 14-06-2025

Volume 1 | Issue 2

Anisotropic Brown Dwarfs Stars with Quadratic Equation of State

Manuel Malaver*[1,2]

[1]Department of Basic Sciences, Maritime University of the Caribbean, Catia la Mar, Venezuela. Email: mmf.umc@gmail.com

[2]Institute of Scholars, Muddhinapalya Bengaluru-560091, Karnataka, India.

***Corresponding author:** Manuel Malaver, Department of Basic Sciences, Maritime University of the Caribbean, Catia la Mar, Venezuela.

Citation: Manuel Malaver (2025) Anisotropic Brown Dwarfs Stars with Quadratic Equation of State. Open Access J Phys & Math. Research article 1(2): 1-9.

Abstract

In this research we found new classes of exact solutions to the Einstein-Maxwell system of equations for anisotropic matter distribution with a particular form of the metric potential and considering a quadratic equation of state, which allows to describe the physical properties as the radial pressure, energy density, anisotropy, mass, surface redshift of a type of stellar objects known as brown dwarfs. The new obtained models are consistent with the limit mass of brown dwarfs 2MASS 0727+1710, 2MASS 0729-3954, DEN 0255-4700 and 2MASS J0348-6022.

Keywords: Anisotropic matter, Metric potential, Quadratic equation of state, Brown dwarfs.

1.Introduction

From the development of Einstein´s theory of general relativity, the modelling of superdense mater configurations is an interesting research area [1,2]. In the last decades, such models allow explain the behavior of massive objects as neutron stars, quasars, pulsars, black holes and white dwarfs [3,4]. Komathiraj and Maharaj [3] find new classes exact solutions to the Einstein-Maxwell system of equations for a charged sphere with a particular choice of the electric field intensity and one of the gravitational potentials [4]. have obtained a class of solutions to the Einstein-Maxwell system assuming a particular choice of the electric field intensity.

In theoretical works of realistic stellar models, it is important to include the pressure anisotropy [5-7]. Bowers and Liang [5] extensively discuss the effect of pressure anisotropy in general relativity. The existence of anisotropy within a star can be explained by the presence of a solid core, phase transitions, a type III super fluid, a pion condensation [6] or another physical phenomena as the presence of an electrical field [7]. The physics of ultrahigh densities is not well understood and many of the strange stars' studies have been performed within the framework of the MIT-Bag model [8].

In this model, the strange matter equation of state has a simple linear form given by $p=\frac{1}{3}(\rho-4B)$ where ρ is the energy density, p is the isotropic pressure and B is the bag constant. Many researchers have used a great variety of mathematical techniques to try to obtain exact solutions for quark stars within the framework of MIT-Bag model: Komathiraj and Maharaj [3] found two new classes of exact solutions to the Einstein-Maxwell system of equations with a particular form of the gravitational potential and isotropic pressure. Malaver [9,10] also has obtained some models for compact stars considering a potential gravitational that depends on an adjustable parameter. Thirukkanesh and Maharaj [11] studied the behavior of compact relativistic objects with anisotropic pressure in the presence of the electromagnetic field [12]. generated new models for quark stars with charged anisotropic matter considering a linear equation of state. Thirukkanesh and Ragel [13] obtained new models for compact stars with quark matter. Sunzu et al. found new classes of solutions with specific forms for the measure of anisotropy [14].

Several mathematical modeling within the framework of the general theory of relativity has been used to explain the behavior and structure of massive objects as neutron stars, quasars, black holes, pulsars and white dwarfs [15-25] and requires finding

the exact solutions of the Einstein-Maxwell system [3]. A detailed and systematic analysis was carried out by Delgaty and Lake [26] which obtained several analytical solutions that can describe realistic stellar configurations. Islam et al. [27] have solved the Einstein-Maxwell field equations and obtained mass-radio relations that allow modelling stellar objects at various regions of Hertzsprung-Russel diagram such as red dwarfs, white dwarfs, red giants, super giants and brown dwarfs.

Within use of Einstein´s field equations, important advances have been made to model the interior of a star. In particular, Feroze and Siddiqui [15,16] and Malaver [17,18] consider a quadratic equation of state for the matter distribution and specify particular forms for the gravitational potential and electric field intensity. Mafa Takisa and Maharaj [19] obtained new exact solutions to the Einstein-Maxwell system of equations with a polytropic equation of state. Thirukkanesh and Ragel [20] have obtained particular models of anisotropic fluids with polytropic equation of state which are consistent with the reported experimental observations. Malaver [21,22] generated new exact solutions to the Einstein-Maxwell system considering Van der Waals modified equation of state with and without polytropical exponent and Thirukkanesh and Ragel [23] presented a anisotropic strange quark matter model by imposing a linear barotropic equation of state with Tolman IV form for the gravitational potential. Mak and Harko [24] found a relativistic model of strange quark star with the suppositions of spherical symmetry and conformal Killing vector.

Brown dwarfs are not really stars, because there is no thermonuclear fusion in their core. These objects are smaller and cooler than stars, but too massive to be considered planets closest stars [28]. Using a quadratic equation of state with a particular metric function and taking pressure anisotropy into account, in this research we developed new mathematical models for a brown dwarfs. This is how the article is structured: we introduce Einstein's field equations for anisotropic fluid distribution in section 2. In section 3, we build novel models for charged anisotropic matter by selecting an electric field strength and gravitational potential that enable the solution of the field equations. The requirements for physical acceptability are covered in Section 4. Section 5 looks at these novel solutions' physical characteristics and validity. Section 6 presents the findings drawn from the outcomes of the computational implementations.

2. Einstein Field Equations

We consider a spherically symmetric, static and homogeneous and anisotropic spacetime in Schwarzschild coordinates given by

$$ds^2 = -e^{2\nu(r)}dt^2 + e^{2\lambda(r)}dr^2 + r^2(d\theta^2 + \sin^2\theta d\phi^2) \quad (1)$$

where $\nu(r)$ and $\lambda(r)$ are two arbitrary functions.

The Einstein field equations for the charged anisotropic matter are given by

$$T_{00} = -\rho - \frac{1}{2}E^2 \quad (2)$$

$$T_{11} = p_r - \frac{1}{2}E^2 \quad (3)$$

$$T_{22} = T_{33} = p_t + \frac{1}{2}E^2 \quad (4)$$

where ρ is the energy density, p_r is the radial pressure, p_t is electric field intensity and p_t is the tangential pressure, respectively. Using the transformations, $x = r^2$, $Z(x) = e^{-2\lambda(r)}$ and $A^2y^2(x) = e^{2\nu(r)}$ with arbitrary constants A and c>0, suggested by Durga pal and Bannerji [29], the metric (1) take the form

$$ds^2 = -e^{2\nu(r)}dt^2 + e^{2\lambda(r)}dr^2 + r^2(d\theta^2 + \sin^2\theta d\phi^2) \quad (5)$$

and the Einstein field equations can be written as

$$\frac{1-Z}{x} - 2\dot{Z} = \frac{\tilde{n}}{c} + \frac{E^2}{2c} \quad (6)$$

$$4Z\frac{\dot{y}}{y} - \frac{1-Z}{x} = \frac{p_r}{c} - \frac{E^2}{2c} \quad (7)$$

$$4Z\frac{\ddot{y}}{y} + (4\dot{Z} + 2\dot{Z})\frac{\dot{y}}{y} + \dot{Z} = \frac{p_t}{c} + \frac{E^2}{2c} \quad (8)$$

$$p_t = p_r + \Delta \quad (9)$$

$$\frac{\Delta}{c} = 4Z\frac{\ddot{y}}{y} + \dot{Z}\left(1 + 2x\frac{\dot{y}}{y}\right) + \frac{1-Z}{x} - \frac{E^2}{c} \quad (10)$$

$$\sigma^2 = \frac{4Z}{x}\left(x\dot{E} + E\right)^2 \quad (11)$$

σ is the charge density and dots denoting differentiation with respect to x. With the transformations of [29], the mass within a radius r of the sphere take the form

$$M(x) = \frac{1}{4^{3/2}} \int_0^x \sqrt{x}\,\tilde{n}(x)dx \quad (12)$$

The interior metric (1) with the charged matter distribution should match the exterior spacetime described by the Reissner-Nordstrom metric:

$$d^2 = -\left(1 - \frac{2M}{r} + \frac{Q^2}{r^2}\right)dt^2 + \left(1 - \frac{2M}{r} + \frac{Q^2}{r^2}\right)^{-1} dr^2 + r^2(d\theta^2 + \sin^2\theta d\phi^2) \quad (13)$$

Where the total mass and the total charge of the star are denoted by M and q^2, respectively. The junction conditions at the stellar surface are obtained by matching the first and the second fundamental forms for the interior metric (1) and the exterior metric (13).

In this paper, we assume the following quadratic equation of state

$$p_r = \alpha\tilde{n}^2 + \beta - \gamma \quad (14)$$

where α , β and γ are arbitrary constants

3. A New Class of Anisotropic Models

In order to solve the Einstein-Maxwell field equations, we take the form of the gravitational potential *Z(x)* as *Z(x) =1-ax* proposed for [30] where a is a real constant. This potential is regular at the origin and well behaved in the interior of the sphere [31] for the electric field intensity, we make the particular choice:

$$\frac{E^2}{2C} = KxZ(x) = Kx(1 - ax) \quad (15)$$

This electric field is finite at the center of the star and remains continuous in the interior. Using Z(x) and eq. (15) in eq. (6), we obtain

$$\rho = C[3a - Kx(1 - ax)] \quad (16)$$

Substituting eq. (16) in eq. (14), the radial pressure can be written in the form:

$$P_r = \alpha C^2[3a - Kx(1 - ax)]^2 + \beta C[3a - Kx(1 - ax)] - \gamma \quad (17)$$

Using eq. (16) in eq. (12), the expression of the mass function is

$$M(x) = \frac{(5aKx^2 - 7Kx + 3a)x^{3/2}}{10\sqrt{C}} \quad (18)$$

With eq. (15) and *Z(x)* in eq. (11), the charge density is

$$\sigma^2 = 8C^2K(2 - 3ax)^2 \quad (19)$$

With the equations (14), (15), (16) and *Z(x)*, eq. (7) becomes:

$$\frac{\dot{y}}{y} = \frac{\alpha C[3a - Kx(1 - ax)]^2}{4(1 - ax)} + \frac{\beta[3a - Kx(1 - ax)]}{4(1 - ax)} - \frac{\gamma}{4C(1 - ax)} - \frac{Kx}{4} + \frac{a}{4(1 - ax)} \quad (20)$$

Integrating eq. (20) we obtain:

$$y(x) = c_1(ax - 1)^{A^*} e^{-\frac{Kx^2(3CKa\alpha x^2 - 4Kx\alpha x + 3C\alpha + 6\beta + 6)}{8}} \quad (21)$$

where for the convenience we have let

$$A^* = \frac{-9\alpha a^2C^2 - (3\beta + 1)aC + \gamma}{4aC} \quad (22)$$

c_1 is the constant of integration

The metric functions $e^{2\lambda}$ and $e^{2\nu}$ can be written as:

$$e^{2\lambda} = \frac{1}{1 - ax} \quad (23)$$

$$e^{2\nu(r)} = A^2c_1^2(ax - 1)^{2A^*} e^{-\frac{Kx^2(3CKa\alpha x^2 - 4Kx\alpha x + 3C\alpha + 6\beta + 6)}{4}} \quad (24)$$

and the anisotropy Δ is given

$$\frac{\Delta}{C} = 4x(1 - ax)\left\{\begin{array}{l} \frac{(A^2 - A)a^2}{(ax - 1)^2} + \frac{2a}{ax - 1}\left[\begin{array}{l} -\frac{Kx}{4}\left(\begin{array}{l} 3CKa\alpha x^2 - 4Kx\alpha x \\ +3C\alpha + 6\beta + 6 \end{array}\right) \\ -\frac{Kx^2}{8}(6CKa\alpha x - 4Kx\alpha) \end{array}\right] \\ -\frac{Kx}{4}(3CKa\alpha x^2 - 4Kx\alpha x + 3C\alpha + 6\beta + 6) \\ -\frac{Kx}{4}(6CKa\alpha x - 4Kx\alpha) - \frac{K^2C\alpha x^2}{8} \\ +\left[\begin{array}{l} -\frac{Kx}{4}(3CKa\alpha x^2 - 4Kx\alpha x + 3C\alpha + 6\beta + 6) \\ -\frac{Kx^2}{8}(6CKa\alpha x - 4Kx\alpha) \end{array}\right]^2 \end{array}\right\}$$

$$-a\left\{1 + 2x\left[\begin{array}{l} \frac{a}{ax - 1} - \frac{Kx}{4}(3CKa\alpha x^2 - 4Kx\alpha x + 3C\alpha + 6\beta + 6) \\ -\frac{Kx^2}{8}(6CKa\alpha x - 4Kx\alpha) \end{array}\right]\right\}$$

$$+a - 2Kx(1 - ax)$$

4. Conditions of Physical Acceptability

For a model to be physically acceptable, the following conditions should be satisfied [26,30]:

1. The metric potentials $e^{2\lambda}$ and $e^{2\nu}$ assume finite values throughoutthe stellar interior and are singularity-free at the center r=0.
2. The energy density ρ should be positive and a decreasing function inside the star.
3. The radial pressure also should be positive and a decreasing function of radial parameter.
4. The radial pressure and density gradients $dP_r/d\rho \le 0$ and $0 \le r \le R$ for $0 \le r \le R$.
5. The anisotropy is zero at the center $r=0$, i.e. $\Delta(r=0)=0$.
6. Any physically acceptable model must satisfy the causality condition, that is, for the radial sound speed $v_{sr}^2 = \frac{dP_r}{d\rho}$,we should have $0 \le v_{sr}^2 \le 1$.
7. The charged interior solution should be matched with the Reissner–Nordström exterior solution, for which the metric is given by

$$ds^2 = -\left(1 - \frac{2M}{r} + \frac{Q^2}{r^2}\right)dt^2 + \left(1 - \frac{2M}{r} + \frac{Q^2}{r^2}\right)^{-1} dr^2 + r^2 d\theta^2 + r^2 \sin^2\theta d\varphi^2$$

The conditions (ii) and (iv) imply that the energy density must reach a maximum at the center and decrease towards the surface of the sphere.

5. Physical Features of the new Models

We now present the analysis of the physical characteristics for the new models. The metric functions $e^{2\lambda}$ and $e^{2\nu}$ have finite values and remain positive throughout the stellar interior. At the center $e^{2\lambda(0)} = 1$ and $e^{2\nu(0)} = A^2 c_1^2 (-1)^{2A^*}$.

We show that in $r=0$ $\left(e^{2\lambda(r)}\right)'_{r=0} = \left(e^{2\nu(r)}\right)'_{r=0} = 0$ and this makes is possible to verify that the gravitational potentials are regular at the center. The energy density and radial pressure are positive and well behaved within the star. Also, we have for the central density and pressure $\rho(0) = 3\alpha C$ and $P_r(0) = 9a^2\alpha C^2 + 3\beta\alpha C - \gamma$.

In the surface of the star $r=R$, we have $(\quad = \quad) = 0$ and

$$R = \frac{\sqrt{2a\alpha K\left(K\ \alpha + \sqrt{-2\ C^2 K\ ^2\alpha^2 + C^2K^2\alpha^2 + 2CKa\alpha\sqrt{4\varphi\ + \beta^2}} - 2CKa\beta\right)}}{2a\alpha K} \quad (26)$$

For a realistic star, it is expected that the gradient of energy density and radial pressure should be decreasing functions of the radial coordinate r. In this model, for all $0 \le r \le R$, we obtain respectively:

$$\frac{d\rho}{d} = -2KCr\left(1 - aCr^2\right) + 2K\ ^2 r^3 a < 0 \quad (27)$$

$$\frac{dP_r}{d} = 2\alpha C^2\left[3a - KCr^2\left(1 - aCr^2\right)\right]\left[-2KCr\left(1 - aCr^2\right) + 2K\ ^2 r^3 a\right] + \beta C\left[-2KCr\left(1 - aCr^2\right) + 2K\ ^2 r^3 a\right] \quad (28)$$

According to the equations (27) and (28), the energy density and radial pressure decrease from the centre to the surface of the star.

The causality condition demands that the radial sound speed defined as $v_s^2 = \frac{dP_r}{\rho}$ should not exceed the speed of light and it must be within the limit $0 \le v_s^2 \le 1$ in the interior of the star [26]. In this model, we have with the transformations of Durgapal and Bannerji [29]:

$$0 \le 6a\alpha C - 2\alpha K\ ^2 r^2 + 2\alpha\alpha K C^3 r^4 + \beta \le 1 \quad (29)$$

On the boundary r=R, the solution must match the Reissner–Nordström exterior space–time and the continuity of e^{ν} and e^{λ} across the boundary $r=R$ is

$$e^{2\nu} = e^{-2\lambda} = 1 - \frac{2M}{R} + \frac{Q^2}{R^2} \quad (30)$$

Then for the matching conditions, we obtain:

$$\frac{2M}{R} = aCR^2 + KCR^4 - aKC^2R^6 \quad (31)$$

and the surface red-shift Z_S can be expressed by the following relation

$$Z_S = \frac{1}{\sqrt{1-\frac{2M(r)}{r}}} - 1 \qquad (32)$$

The figures 1,2,3,4,5,6,7,8, 9 and 10 represent the plots of $\frac{E^2}{2C}$, σ^2 , ρ , P_r , Z_S, v_s^2 , $\frac{d\rho}{dl}$, $\frac{dP_r}{dl}$, M and Δ with the radial coordinate. In every graph we looked at $C=1$ and a=0.0003.

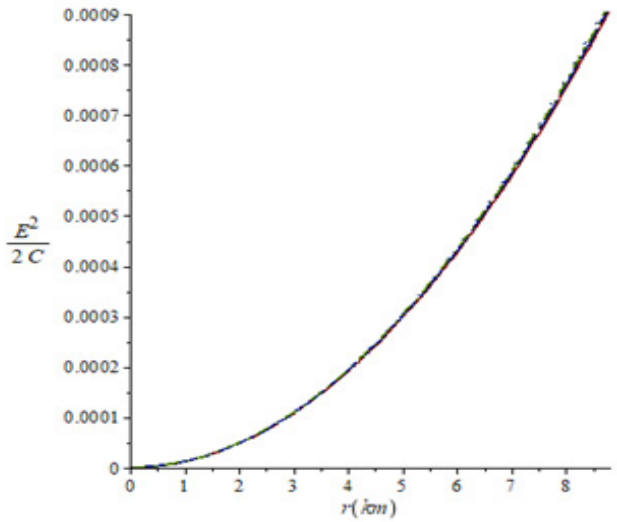

Figure 1. Electric field intensity against the radial coordinate for K=0.000012 (solid line), K=0.0000121 (longdash line), K=0.0000122 (dashdot line) and K=0.0000123 (spacedot ine). For all the cases a=0.0003.

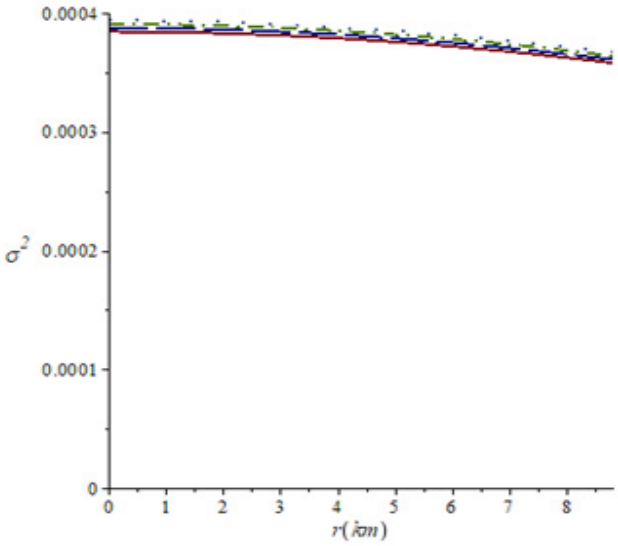

Figure 2. Charge density against the radial coordinate for K=0.000012 (solid line), K=0.0000121 (longdash line), K=0.0000122 (dashdot line) and K=0.0000123 (spacedot line). For all the cases a=0.0003

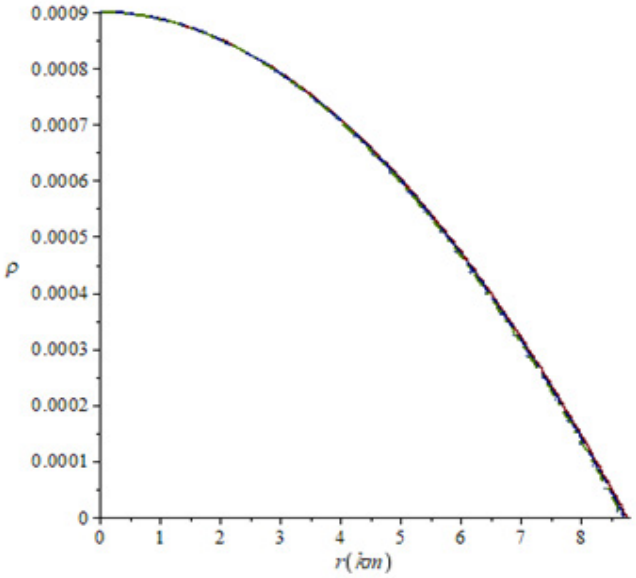

Figure 3. Energy density against the radial parameter for K=0.000012 (solid line), K=0.0000121 (longdash line), K=0.0000122 (dashdot line) and K=0.0000123 (spacedot line). For all the cases a=0.0003.

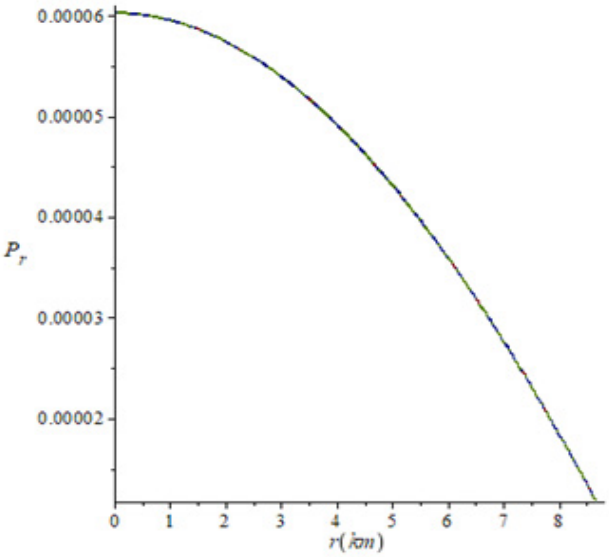

Figure 4. Radial pressure against the radial parameter for K=0.000012 (solid line), K=0.0000121 (longdash line), K=0.0000122 (dashdot line) and K=0.0000123 (spacedot line). For all the cases a=0.0003.

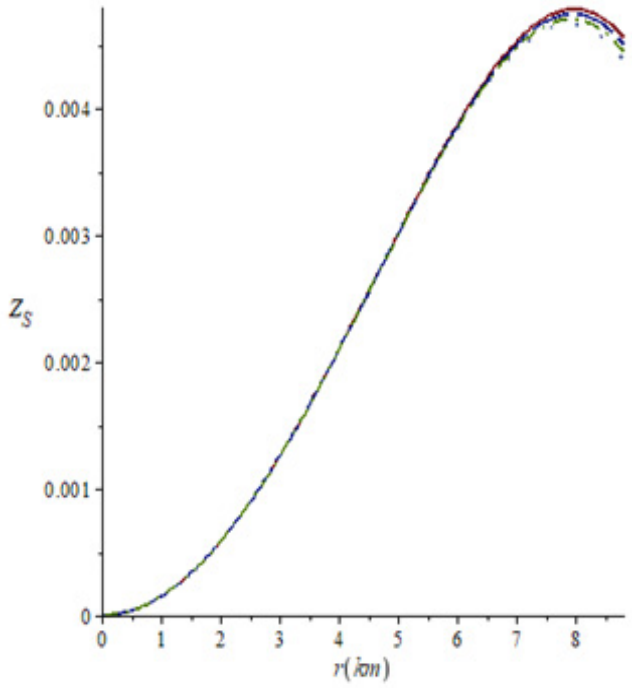

Figure 5. Surface red-shift against the radial parameter for K=0.000012 (solid line), K=0.0000121 (longdash line), K=0.0000122 (dashdot line) and K=0.0000123 (spacedot line). For all the cases a=0.0003

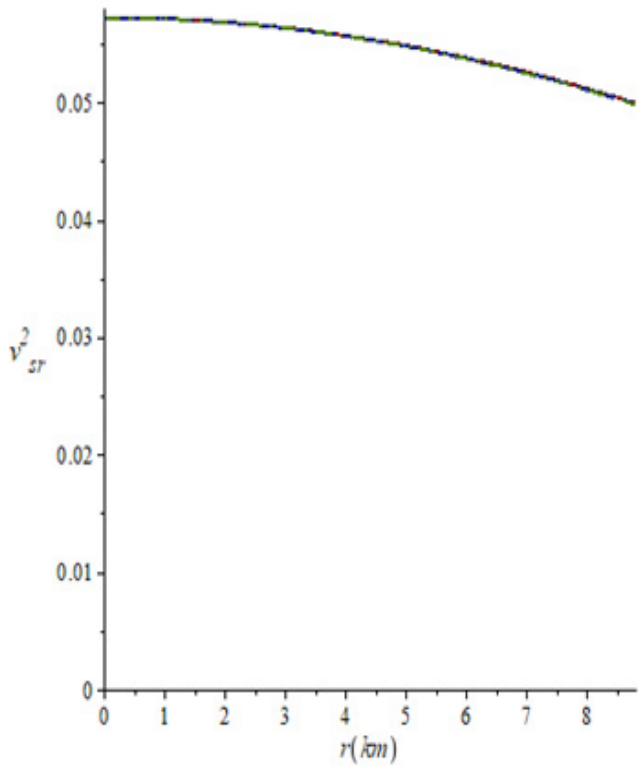

Figure 6. Radial speed sound v_s^2 against the radial parameter for K=0.000012 (solid line), K=0.0000121 (longdash line), K=0.0000122 (dashdot line) and K=0.0000123 (spacedot line). For all the cases a=0.0003

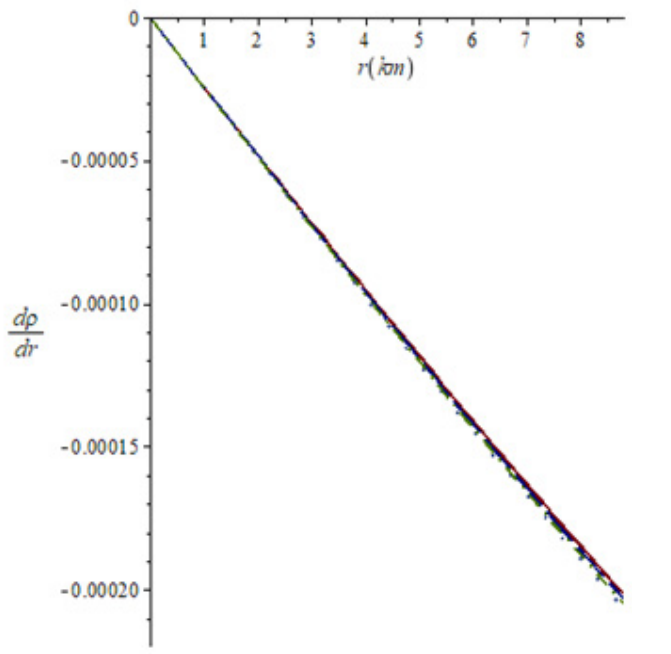

Figure 7. Energy density gradient against the radial parameter for K=0.000012 (solid line), K=0.0000121 (longdash line), K=0.0000122 (dashdot line) and K=0.0000123 (spacedot line). For all the cases a=0.0003

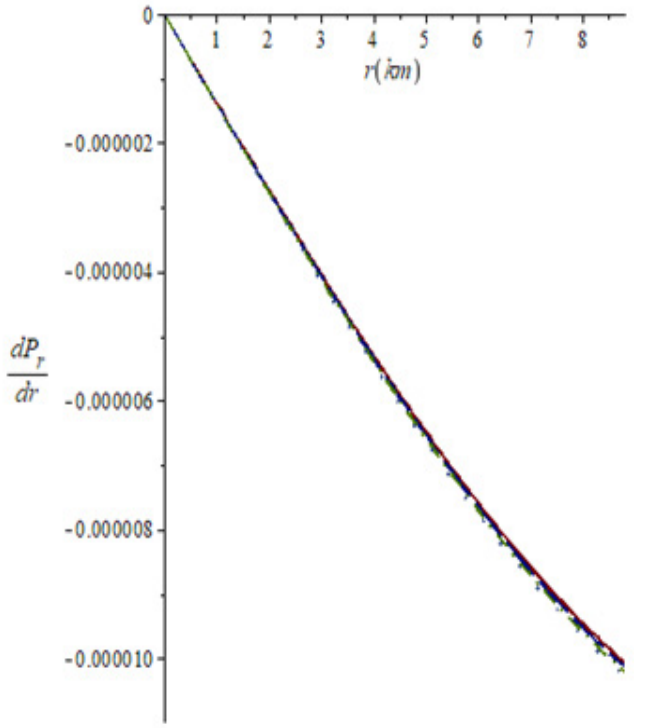

Figure 8. Radial pressure gradient against the radial parameter for K=0.000012 (solid line), K=0.0000121 (longdash line), K=0.0000122 (dashdot line) and K=0.0000123 (spacedot line). For all the cases a=0.0003

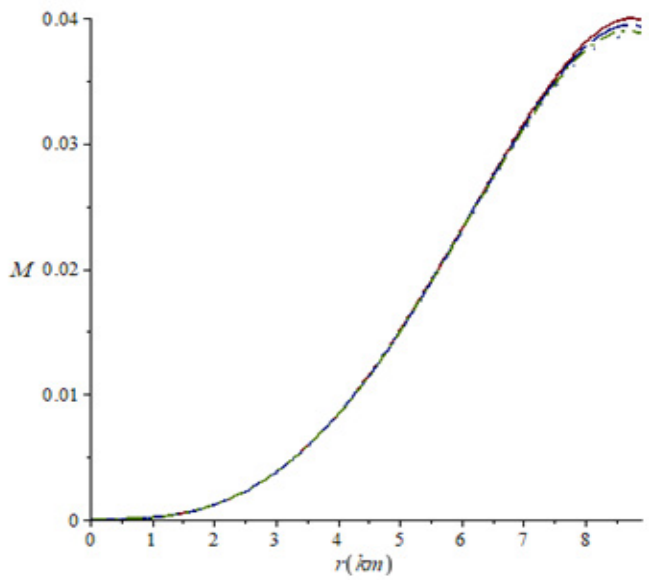

Figure 9. Mass function against the radial parameter for K=0.000012 (solid line), K=0.0000121 (longdash line), K=0.0000122 (dashdot line) and K=0.0000123 (spacedot line). For all the cases a=0.0003

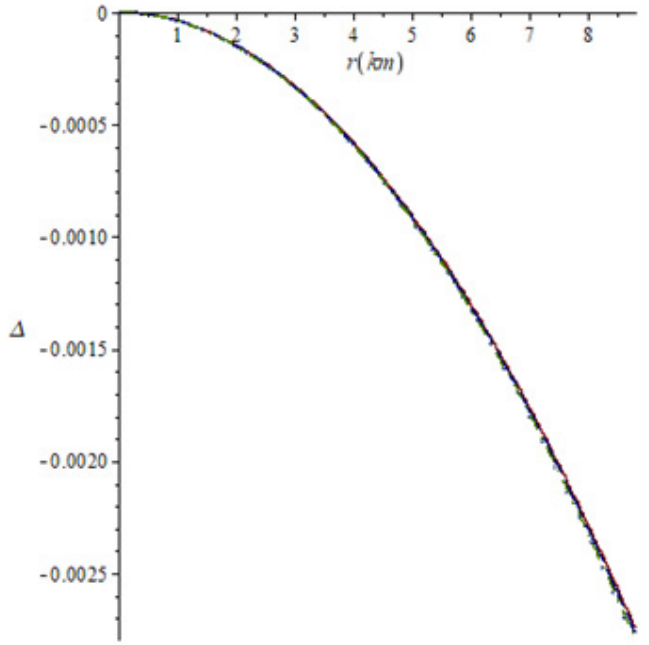

Figure 10. Anisotropy against the radial parameter for K=0.000012 (solid line), K=0.0000121 (longdash line), K=0.0000122 (dashdot line) and K=0.0000123 (spacedot line). For all the cases a=0.0003

In Figure 1 is noted that the electric field intensity stays positive, continuous, and increases monotonically throughout the stellar interior and the charge density is a function that steadily drops, as shown in Figure 2. The energy density remains positive, continuous and is monotonically decreasing function throughout the interior of the star as depicted in the Figure 3 for all values of K considered. The radial pressure is non negative and is a decreasing function with the radial parameter as shown in Figure 4. Figure 5 also displays the surface red-shift profiles for all the values of K, demonstrating that the surface red-shift likewise displays the desired behavior within the stellar model. In figure 6, we note that v_r^2 within the desired range $0 \leq v_r^2 \leq 1$ for all the values of K. The figures 7 and 8 respectively show that the gradients of density and radial pressure are decreasing throughout the star. The mass function in Figure 11 is continuous, increasing, takes finite values, and behaves well in the interior of the star for a range of K values taken into consideration The anisotropic component Δ, as plotted in Figure 10, vanishes at the center of the star, or Δ(r=0)=0 and is continuously decreasing.

The reported and calculated masses of four brown dwarfs stars and calculated values of Z_s with the selected values of K are given in Table 1.

Table 1. Observed and calculated values of stellar masses, surface redshift Z_s and the chosen K parameter for four candidates to brown dwarfs with a=0.0003

Brown Dwarfs	Values of K	Reported mass $M(M_\odot)$	Calculated mass $M(M_\odot)$	Calculated Z_s
2MASS 0727 + 1710	0.0000120	0.04	0.03994385	0.004570214
2MASS J0348 -6022	0.0000121	0.04	0.03942488	0.004510433
DEN 0255-4700	0.0000122	0.04	0.03890590	0.004450662
2MASS 0729 -3954	0.0000123	0.035	0.03838693	0.004390902

$M_\odot$ = sun's mass

We can compare the values calculated for the mass function with experimental data. We found that the calculated masses are very similar to $0.04M_{\odot}$. For K=0.000012 the values of a and K allow us to obtain a mass of $0.03994385M_{\odot}$ which can correspond to astronomic object 2MASS 0727 + 1710 [32]. With K=0.0000121, the resulting mass is very similar to brown dwarf 2MASS J0348 - 6022 whose observed mass is $0.04M_{\odot}$ and the values of the parameters a=0.0003 and K=0.0000122 also generate the mass $0.04M_{\odot}$ that can correspond to the stellar object DEN 0255 - 4700 [33]. The brown dwarf 2MASS J0348 - 6022 is the fastest-rotating brown dwarf confirmed as of 2022 [34] and DEN 0255-4700 is the faintest brown dwarf with a low visible magnitude [35]. For the case K=0.0000123 we obtained a comparable mass with the star 2MASS 0729 -3954 located 26 light years away from the sun and is a single star of spectral class T8 D [36]. In all the cases, the surface red-shift is a continuous, monotonically increasing function with radial coordinate in every instance, reaching its maximum value Z_S =0.004570214 for K= 0.000012, which is consistent with the astronomical bodies studied for Islam et al. [27].

6. Conclusion

In this work, we solved Einstein-Maxwell field equations to construct some simple relativistic charged star models for a static spherically symmetric locally anisotropic fluid distribution. By choosing a metric potential, figuring out the electric charge distribution, and applying the quadratic equation of state, we have investigated the behavior of fluid distribution. An analytical stellar model with such physical properties could be very helpful in explaining the internal structure of electrically charged stars. The newly found models are in perfect agreement with the Reissner–Nordström exterior metric across the boundary $r=R$, since matter variables and the gravitational potentials of this study are compatible with the physical analysis of these stars.

The suggested model operates well and may be compared with of brown dwarfs 2MASS 0727+1710, 2MASS 0729-3954, DEN 0255-4700 and 2MASS J0348-6022 according to plots created and physical properties pertaining to matter, radial pressure, density, anisotropy, surface redshift and charge density. Although the brown dwarfs are not as huge as the least massive main-sequence stars, they are nevertheless large enough to release some heat and light from the fusion of deuterium, and they have more mass than the largest gas giant planets overall.

Our current method's specific goal is to show that we can reconstruct the models of different astronomic objects that are consistent with the available observational data by selecting the right constant parameters. As a result, for academics working in this area, the models examined in this paper may have substantial astrophysical significance.

References

1. Kuhfitting PKF (2011) Some remarks on exact wormhole solutions. Adv. Studies Theor. Phys 5(8): 365- 370.
2. Schwarzschild K (1916) On the gravitational field of a sphere of incompressible fluid according to Einstein's theory. Math Phys Tech, pp: 424-434.
3. Komathiraj K, Maharaj SD (2008) Classes of exact Einstein-Maxwell solutions, Gen Rel Grav 39: 2079-2093.
4. Sharma R, Mukherjee S, Maharaj SD (2001) General solution for a class of static charged Spheres. General Relativity and Gravitation 33: 999- 1009.
5. Bowers RL, Liang EPT (1974) Anisotropic Spheres in General Relativity. Astrophys J 188: 657-665.
6. Sokolov AI (1980) Phase transitions in a superfluid neutron liquid. Sov Phys JETP 52: 575.
7. Usov VV (2004) Electric fields at the quark surface of strange stars in the color-flavor locked phase. Phys Rev 70: 067301.
8. Komathiraj K, Maharaj SD (2007) Analytical models for quark stars. Int J Mod Phys 16: 1803-1811. 61
9. Malaver M, Iyer R (2022) Analytical Model of Compact Star with a New Version of Modified Chaplygin Equation of State, Applied Physics 5(1): 18-36.
10. Malaver M, Iyer R (2023) Charged Stellar Model with Generalized Chaplygin Equation of State Consistent with Observational Data. Universal Journal of Physics Research 2(1): 43-59.
11. Thirukkanesh S, Maharaj SD (2008) Charged anisotropic matter with linear equation of state, Class. Quantum Gravity 25: 235001.
12. Maharaj SD, Sunzu JM, Ray S (2014) Some Simple Models for Quark Stars. The European Physical Journal Plus 129(3).
13. Thirukkanesh S, Ragel FC (2013) A class of exact strange quark star model. PRAMANA-Journal of physics 81(2): 275-286.
14. Sunzu JM, Maharaj SD, Ray S (2014) Quark star model with charged anisotropic matter. Astrophysics. Space. Sci

354: 517-524.

15. Feroze T, Siddiqui A (2011) Charged anisotropic matter with quadratic equation of state. General Relativity and Gravitation 43: 1025-1035.
16. Feroze T, Siddiqui A (2014) Some exact solutions of the Einstein- Maxwell equations with a quadratic equation of state. Journal of the Korean Physical Society 65: 944-947.
17. Malaver M (2014) Strange Quark Star Model with Quadratic Equation of State, Frontiers of Mathematics and Its Applications 1: 9-15.
18. Malaver M (2015) Relativistic Modeling of Quark Stars with Tolman IV Type Potential. International Journal of Modern Physics and Application 2: 1-6.
19. Takisa PM, Maharaj SD (2013) Some charged polytropic models. General Relativity and Gravitation, 45: 1951-1969.
20. Thirukkanesh S, Ragel FC (2012) Exact anisotropic sphere with polytropic equation of state. PRAMANA-Journal of physics 78: 687- 696.
21. Malaver M (2013) Analytical model for charged polytropic stars with Van der Waals Modified Equation of State. American Journal of Astronomy and Astrophysics 1: 41-46.
22. Malaver M (2013) Regular model for a quark star with Van der Waals modified equation of state. World Applied Programming 3: 309-313.
23. Thirukkanesh S, Ragel FC (2014) Strange star model with Tolmann IV type potential. Astrophysics and Space Science 352: 743-749.
24. Mak MK, Harko T (2004) Quark stars admitting a one-parameter group of conformal motions. Int. J. Mod. Phys. D 13: 149-156.
25. Malaver M, Iyer R (2024) Modelling of Charged Dark Energy Stars in a Tolman IV Spacetime. Open Access Journal of Astronomy 2: 1-12.
26. Delgaty MSR, Lake K (1998) Physical Acceptability of Isolated, Static, Spherically Symmetric, Perfect Fluid Solutions of Einstein's Equations. Comput Phys Commun 115: 395.
27. Islam, S, Datta, S., Das, T. K. A parametric model to study the mass radius relationship of stars. https://arxiv.org/abs/1702.05171
28. https://www.stellarcatalog.com/
29. Durgapal MC, Bannerji R. New analytical stellar model in general relativity. Phys.Rev. D. 1983; 27: 328-331.
30. Malaver M (2014) Strange Quark Star Model with Quadratic Equation of State, Frontiers of Mathematics and Its Applications 1: 9-15.
31. Lighuda AS, Sunzu JM, Maharaj SD, Mureithi EW (2021) Charged stellar model with three layers. Res Astron Astrophys, 21: 310.
32. Sorahana S, Yamamura I, Murakami H (2013) On the Radii of Brown Dwarfs Measured with AKARI Near-Infrared Spectroscopy. https://arxiv.org/abs/1304.1259
33. Burgasser AJ (2008) Brown dwarfs: Failed stars, super Jupiters. Physics Today.
34. Wilson PA, Rajan A, Patience J (2014) The brown dwarf atmosphere monitoring (BAM) project I. The largest near-IR monitoring survey of L and T dwarfs. https://arxiv.org/abs/1404.4633
35. Vallenari A. et al. (Gaia collaboration) (2023). Gaia Data Release 3. Summary of the content and survey properties. https://arxiv.org/abs/2208.00211
36. Lopper D, Kirkpatrick, Burgasser AJ(2007) Discovery of 11 New T Dwarfs in the Two Micron All-Sky Survey, Including a Possible L/T Transition Binary. https://arxiv.org/abs/0706.1601.